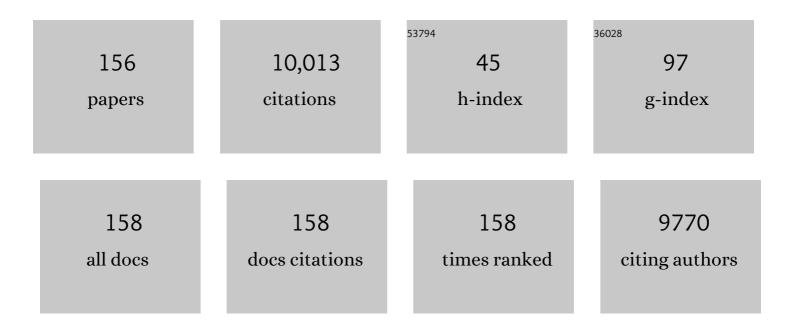
## List of Publications by Year in descending order

Source: https://exaly.com/author-pdf/1371201/publications.pdf Version: 2024-02-01



#	Article	IF	CITATIONS
1	Consensus Nomenclature for in vivo Imaging of Reversibly Binding Radioligands. Journal of Cerebral Blood Flow and Metabolism, 2007, 27, 1533-1539.	4.3	1,840
2	A doubleâ€blind controlled trial of bilateral fetal nigral transplantation in Parkinson's disease. Annals of Neurology, 2003, 54, 403-414.	5.3	1,450
3	Expectation and Dopamine Release: Mechanism of the Placebo Effect in Parkinson's Disease. Science, 2001, 293, 1164-1166.	12.6	885
4	Levodopa-induced changes in synaptic dopamine levels increase with progression of Parkinson's disease: implications for dyskinesias. Brain, 2004, 127, 2747-2754.	7.6	361
5	Dopamine release in human ventral striatum and expectation of reward. Behavioural Brain Research, 2002, 136, 359-363.	2.2	303
6	PET in LRRK2 mutations: comparison to sporadic Parkinson's disease and evidence for presymptomatic compensation. Brain, 2005, 128, 2777-2785.	7.6	242
7	Ageâ€specific progression of nigrostriatal dysfunction in Parkinson's disease. Annals of Neurology, 2011, 69, 803-810.	5.3	197
8	Randomized trial of intermittent intraputamenal glial cell line-derived neurotrophic factor in Parkinson's disease. Brain, 2019, 142, 512-525.	7.6	194
9	NEMA NU 4-2008 Comparison of Preclinical PET Imaging Systems. Journal of Nuclear Medicine, 2012, 53, 1300-1309.	5.0	191
10	Technical performance evaluation of a human brain PET/MRI system. European Radiology, 2012, 22, 1776-1788.	4.5	140
11	Longitudinal evolution of compensatory changes in striatal dopamine processing in Parkinson's disease. Brain, 2011, 134, 3290-3298.	7.6	133
12	Accurate Event-Driven Motion Compensation in High-Resolution PET Incorporating Scattered and Random Events. IEEE Transactions on Medical Imaging, 2008, 27, 1018-1033.	8.9	132
13	PET performance measurements using the NEMA NU 2-2001 standard. Journal of Nuclear Medicine, 2002, 43, 1398-409.	5.0	130
14	PET Study of [18F]6-Fluoro-l-Dopa Uptake in Neuroleptic- and Mood-Stabilizer-Naive First-Episode Nonpsychotic Mania: Effects of Treatment With Divalproex Sodium. American Journal of Psychiatry, 2002, 159, 768-774.	7.2	123
15	Increase in Dopamine Turnover Occurs Early in Parkinson's Disease: Evidence from a New Modeling Approach to PET 18F-Fluorodopa Data. Journal of Cerebral Blood Flow and Metabolism, 2002, 22, 232-239.	4.3	117
16	Dopamine turnover increases in asymptomatic <i>LRRK2</i> mutations carriers. Movement Disorders, 2010, 25, 2717-2723.	3.9	103
17	Advances in imaging in Parkinson's disease. Lancet Neurology, The, 2011, 10, 987-1001.	10.2	99
18	Exercise increases caudate dopamine release and ventral striatal activation in Parkinson's disease. Movement Disorders, 2019, 34, 1891-1900.	3.9	99

#	Article	IF	CITATIONS
19	Serotonin and dopamine transporter PET changes in the premotor phase of LRRK2 parkinsonism: cross-sectional studies. Lancet Neurology, The, 2017, 16, 351-359.	10.2	96
20	Extended Treatment with Glial Cell Line-Derived Neurotrophic Factor in Parkinson's Disease. Journal of Parkinson's Disease, 2019, 9, 301-313.	2.8	89
21	Design and Performance of a Resistor Multiplexing Readout Circuit for a SiPM Detector. IEEE Transactions on Nuclear Science, 2013, 60, 1541-1549.	2.0	87
22	PET Study of the Effects of Valproate on Dopamine D2Receptors in Neuroleptic- and Mood-Stabilizer-Naive Patients With Nonpsychotic Mania. American Journal of Psychiatry, 2002, 159, 1718-1723.	7.2	86
23	Biochemical variations in the synaptic level of dopamine precede motor fluctuations in Parkinson's disease: PET evidence of increased dopamine turnover. Annals of Neurology, 2001, 49, 298-303.	5.3	85
24	Homozygous alpha-synuclein p.A53V in familial Parkinson's disease. Neurobiology of Aging, 2017, 57, 248.e7-248.e12.	3.1	83
25	Changes of Dopamine Turnover in the Progression of Parkinson's Disease as Measured by Positron Emission Tomography: Their Relation to Disease-Compensatory Mechanisms. Journal of Cerebral Blood Flow and Metabolism, 2004, 24, 869-876.	4.3	81
26	Dorsal Striatal D <sub>2</sub> -Like Receptor Availability Covaries with Sensitivity to Positive Reinforcement during Discrimination Learning. Journal of Neuroscience, 2011, 31, 7291-7299.	3.6	81
27	Age-related differences in levodopa dynamics in Parkinson's: implications for motor complications. Brain, 2006, 129, 1050-1058.	7.6	76
28	Effect of electroconvulsive therapy on brain 5-HT <sub>2</sub> receptors in major depression. British Journal of Psychiatry, 2010, 196, 474-479.	2.8	76
29	Improved prediction of outcome in Parkinson's disease using radiomics analysis of longitudinal DAT SPECT images. NeuroImage: Clinical, 2017, 16, 539-544.	2.7	76
30	Robust graft survival and normalized dopaminergic innervation do not obligate recovery in a <scp>P</scp> arkinson disease patient. Annals of Neurology, 2017, 81, 46-57.	5.3	72
31	Irrational Choice under Uncertainty Correlates with Lower Striatal D <sub>2/3</sub> Receptor Binding in Rats. Journal of Neuroscience, 2012, 32, 15450-15457.	3.6	69
32	A Reversible Tracer Analysis Approach to the Study of Effective Dopamine Turnover. Journal of Cerebral Blood Flow and Metabolism, 2001, 21, 469-476.	4.3	67
33	[11C]DTBZ-PET correlates of levodopa responses in asymmetric Parkinson's disease. Brain, 2003, 126, 2648-2655.	7.6	63
34	PBB3 imaging in Parkinsonian disorders: Evidence for binding to tau and other proteins. Movement Disorders, 2017, 32, 1016-1024.	3.9	62
35	Anterior brain glucose hypometabolism predates dementia in progranulin mutation carriers. Neurology, 2013, 81, 1322-1331.	1.1	60
36	<i>DNAJC12</i> and dopaâ€responsive nonprogressive parkinsonism. Annals of Neurology, 2017, 82, 640-646.	5.3	60

#	Article	IF	CITATIONS
37	Application of texture analysis to DAT SPECT imaging: Relationship to clinical assessments. NeuroImage: Clinical, 2016, 12, e1-e9.	2.7	59
38	Positron emission tomography after fetal transplantation in Huntington's disease. Annals of Neurology, 2005, 58, 331-337.	5.3	57
39	The effect of LRRK2 mutations on the cholinergic system in manifest and premanifest stages of Parkinson's disease: a cross-sectional PET study. Lancet Neurology, The, 2018, 17, 309-316.	10.2	57
40	Apomorphine-Induced Changes in Synaptic Dopamine Levels: Positron Emission Tomography Evidence for Presynaptic Inhibition. Journal of Cerebral Blood Flow and Metabolism, 2001, 21, 1151-1159.	4.3	52
41	Visualizing vesicular dopamine dynamics in Parkinson's disease. Synapse, 2009, 63, 713-716.	1.2	50
42	Dopamine transporter relation to levodopaâ€derived synaptic dopamine in a rat model of Parkinson's: an <i>in vivo</i> imaging study. Journal of Neurochemistry, 2009, 109, 85-92.	3.9	50
43	Performance of a PET Insert for High-Resolution Small-Animal PET/MRI at 7 Tesla. Journal of Nuclear Medicine, 2018, 59, 536-542.	5.0	49
44	Lack of Regional Selectivity During the Progression of Parkinson Disease. Archives of Neurology, 2004, 61, 1920-5.	4.5	47
45	Dopamine transporter PET in normal aging: Dopamine transporter decline and its possible role in preservation of motor function. Synapse, 2010, 64, 146-151.	1.2	46
46	First Results From a High-Resolution Small Animal SiPM PET Insert for PET/MR Imaging at 7T. IEEE Transactions on Nuclear Science, 2016, 63, 2424-2433.	2.0	45
47	Trials of neuroprotective therapies for Parkinson's disease: Problems and limitations. Parkinsonism and Related Disorders, 2010, 16, 365-369.	2.2	44
48	In Vivo Measurement of Density and Affinity of the Monoamine Vesicular Transporter in a Unilateral 6-Hydroxydopamine Rat Model of PD. Journal of Cerebral Blood Flow and Metabolism, 2007, 27, 1407-1415.	4.3	40
49	Habitual exercisers versus sedentary subjects with Parkinson's Disease: Multimodal PET and fMRI study. Movement Disorders, 2018, 33, 1945-1950.	3.9	37
50	Optimized machine learning methods for prediction of cognitive outcome in Parkinson's disease. Computers in Biology and Medicine, 2019, 111, 103347.	7.0	37
51	Performance Assessment of a Preclinical PET Scanner with Pinhole Collimation by Comparison to a Coincidence-Based Small-Animal PET Scanner. Journal of Nuclear Medicine, 2014, 55, 1368-1374.	5.0	36
52	<sup>18</sup> F-5-Fluoroaminosuberic Acid as a Potential Tracer to Gauge Oxidative Stress in Breast Cancer Models. Journal of Nuclear Medicine, 2017, 58, 367-373.	5.0	36
53	Quantitative PET in the 2020s: a roadmap. Physics in Medicine and Biology, 2021, 66, 06RM01.	3.0	36
54	Levodopa and pramipexole effects on presynaptic dopamine PET markers and estimated dopamine release. European Journal of Nuclear Medicine and Molecular Imaging, 2010, 37, 2364-2370.	6.4	34

#	Article	IF	CITATIONS
55	Age and severity of nigrostriatal damage at onset of Parkinson's disease. Synapse, 2003, 47, 152-158.	1.2	33
56	<i>In-vivo</i> Measurement of LDOPA Uptake, Dopamine Reserve and Turnover in the Rat Brain Using [ <sup>18</sup> F]FDOPA PET. Journal of Cerebral Blood Flow and Metabolism, 2013, 33, 59-66.	4.3	33
57	Abnormal Metabolic Brain Networks in a Nonhuman Primate Model of Parkinsonism. Journal of Cerebral Blood Flow and Metabolism, 2012, 32, 633-642.	4.3	32
58	Behavioral Deficits and Striatal DA Signaling in LRRK2 p.G2019S Transgenic Rats: A Multimodal Investigation Including PET Neuroimaging. Journal of Parkinson's Disease, 2014, 4, 483-498.	2.8	32
59	Machine learning methods for optimal prediction of motor outcome in Parkinson's disease. Physica Medica, 2020, 69, 233-240.	0.7	32
60	The Nature of Progression in Parkinson's Disease: An Application of Non-Linear, Multivariate, Longitudinal Random Effects Modelling. PLoS ONE, 2013, 8, e76595.	2.5	30
61	System matrix modelling of externally tracked motion. Nuclear Medicine Communications, 2008, 29, 574-581.	1.1	29
62	Noninvasive Nuclear Imaging Enables the In Vivo Quantification of Striatal Dopamine Receptor Expression and Raclopride Affinity in Mice. Journal of Nuclear Medicine, 2011, 52, 1133-1141.	5.0	29
63	Artificial Neural Network–Based Prediction of Outcome in Parkinson's Disease Patients Using DaTscan SPECT Imaging Features. Molecular Imaging and Biology, 2019, 21, 1165-1173.	2.6	29
64	Evaluation of High Density Pixellated Crystal Blocks With SiPM Readout as Candidates for PET/MR Detectors in a Small Animal PET Insert. IEEE Transactions on Nuclear Science, 2012, 59, 1791-1797.	2.0	28
65	[11C]PBR28 PET Imaging is Sensitive to Neuroinflammation in the Aged Rat. Journal of Cerebral Blood Flow and Metabolism, 2015, 35, 1331-1338.	4.3	26
66	Cerebral serotonin transporter measurements with [ <sup>11</sup> C]DASB: A review on acquisition and preprocessing across 21 PET centres. Journal of Cerebral Blood Flow and Metabolism, 2019, 39, 210-222.	4.3	25
67	Investigation of serotonergic Parkinson's disease-related covariance pattern using [11C]-DASB/PET. NeuroImage: Clinical, 2018, 19, 652-660.	2.7	23
68	Brain serotonin-2 receptors in acute mania. British Journal of Psychiatry, 2010, 196, 47-51.	2.8	21
69	Development of a PET Scanner for Simultaneously Imaging Small Animals with MRI and PET. Sensors, 2014, 14, 14654-14671.	3.8	21
70	Joint pattern analysis applied to PET DAT and VMAT2 imaging reveals new insights into Parkinson's disease induced presynaptic alterations. NeuroImage: Clinical, 2019, 23, 101856.	2.7	21
71	Positron emission tomography kinetic modeling algorithms for small animal dopaminergic system imaging. Synapse, 2010, 64, 200-208.	1.2	20
72	Clinical, positron emission tomography, and pathological studies of DNAJC13 p.N855S Parkinsonism. Movement Disorders, 2014, 29, 1684-1687.	3.9	20

#	Article	IF	CITATIONS
73	In vivo quantification of dopamine transporters in mice with unilateral 6-OHDA lesions using [11C]methylphenidate and PET. NeuroImage, 2012, 59, 2413-2422.	4.2	19
74	Incorporating HYPR de-noising within iterative PET reconstruction (HYPR-OSEM). Physics in Medicine and Biology, 2017, 62, 6666-6687.	3.0	19
75	Synthesis and targeting of gold-coated 177Lu-containing lanthanide phosphate nanoparticles—A potential theranostic agent for pulmonary metastatic disease. APL Bioengineering, 2018, 2, 016101.	6.2	19
76	Novel spatial analysis method for PET images using 3D moment invariants: Applications to Parkinson's disease. NeuroImage, 2013, 68, 11-21.	4.2	18
77	Scanning rats on the high resolution research tomograph (HRRT): A comparison study with a dedicated microâ€PET. Medical Physics, 2012, 39, 5073-5083.	3.0	17
78	Cerebral Amyloid-β Deposition Is Associated with Impaired Gait Speed and Lower Extremity Function. Journal of Alzheimer's Disease, 2019, 71, S41-S49.	2.6	17
79	Single Inflammatory Trigger Leads to Neuroinflammation in LRRK2 Rodent Model without Degeneration of Dopaminergic Neurons. Journal of Parkinson's Disease, 2019, 9, 121-139.	2.8	17
80	FDG-PET in presymptomatic C9orf72 mutation carriers. NeuroImage: Clinical, 2021, 31, 102687.	2.7	16
81	An Analytical Scatter Correction for Singles-Mode Transmission Data in PET. IEEE Transactions on Medical Imaging, 2008, 27, 402-412.	8.9	15
82	In Vivo Dopamine Transporter Imaging in a Unilateral 6-Hydroxydopamine Rat Model of Parkinson Disease Using <sup>11</sup> C-Methylphenidate PET. Journal of Nuclear Medicine, 2012, 53, 813-822.	5.0	15
83	In vivo dopaminergic and serotonergic dysfunction in <i>DCTN1</i> gene mutation carriers. Movement Disorders, 2014, 29, 1197-1201.	3.9	15
84	Exploring the use of shape and texture descriptors of positron emission tomography tracer distribution in imaging studies of neurodegenerative disease. Journal of Cerebral Blood Flow and Metabolism, 2016, 36, 1122-1134.	4.3	15
85	The Use of Random Forests to Classify Amyloid Brain PET. Clinical Nuclear Medicine, 2019, 44, 784-788.	1.3	15
86	Dynamic PET image reconstruction utilizing intrinsic dataâ€driven HYPR4D denoising kernel. Medical Physics, 2021, 48, 2230-2244.	3.0	15
87	Imaging striatal dopaminergic function in <i>Phospholipase A2 Group VI</i> –related parkinsonism. Movement Disorders, 2012, 27, 1698-1699.	3.9	14
88	A scan without evidence is not evidence of absence: Scans without evidence of dopaminergic deficit in a symptomatic leucine-rich repeat kinase 2 mutation carrier. Movement Disorders, 2016, 31, 405-409.	3.9	14
89	Data-driven, voxel-based analysis of brain PET images: Application of PCA and LASSO methods to visualize and quantify patterns of neurodegeneration. PLoS ONE, 2018, 13, e0206607.	2.5	14
90	Investigation of Subject Motion Encountered During a Typical Positron Emission Tomography Scan. , 2006, , .		13

#	Article	IF	CITATIONS
91	A Scatter Calibration Technique for Dynamic Brain Imaging in High Resolution PET. IEEE Transactions on Nuclear Science, 2010, 57, 225-233.	2.0	13
92	Serotonergic System Impacts Levodopa Response in Early Parkinson's and Future Risk of Dyskinesia. Movement Disorders, 2021, 36, 389-397.	3.9	13
93	The influence of measurement uncertainties on the evaluation of the distribution volume ratio and binding potential in rat studies on a microPET® R4: a phantom study. Physics in Medicine and Biology, 2005, 50, 2859-2869.	3.0	12
94	Imaging DA release in a rat model of L-DOPA-induced dyskinesias: A longitudinal in vivo PET investigation of the antidyskinetic effect of MDMA. NeuroImage, 2012, 63, 423-433.	4.2	12
95	188Re image performance assessment using small animal multi-pinhole SPECT/PET/CT system. Physica Medica, 2017, 33, 26-37.	0.7	12
96	The Use of Random Forests to Identify Brain Regions on Amyloid and FDG PET Associated With MoCA Score. Clinical Nuclear Medicine, 2020, 45, 427-433.	1.3	12
97	Frameâ€ŧoâ€frame image realignment assessment tool for dynamic brain positron emission tomography. Medical Physics, 2011, 38, 773-781.	3.0	10
98	Application of HDMI® cables as an MRI compatible single cable solution for Readout and power supply of SiPM based PET detectors. , 2012, , .		10
99	PET Image Reconstruction and Deformable Motion Correction Using Unorganized Point Clouds. IEEE Transactions on Medical Imaging, 2017, 36, 1263-1275.	8.9	10
100	A Positron Emission Tomography Study of Norepinephrine Transporter Occupancy and Its Correlation with Symptom Response in Depressed Patients Treated with Quetiapine XR. International Journal of Neuropsychopharmacology, 2018, 21, 108-113.	2.1	10
101	Evaluation of high density pixilated crystal blocks with SiPM readout as candidates for PET/MR detectors in a small animal PET insert. , 2011, , .		9
102	Exploring the effects of coexisting amyloid in subcortical vascular cognitive impairment. BMC Neurology, 2015, 15, 197.	1.8	9
103	Use of Generative Disease Models for Analysis and Selection of Radiomic Features in PET. IEEE Transactions on Radiation and Plasma Medical Sciences, 2019, 3, 178-191.	3.7	9
104	A Monte Carlo approach for improving transient dopamine release detection sensitivity. Journal of Cerebral Blood Flow and Metabolism, 2021, 41, 116-131.	4.3	8
105	Development and biological evaluation of[18F]FMN3PA & [18F]FMN3PU for leucine-rich repeat kinase 2 (LRRK2) inÂvivo PET imaging. European Journal of Medicinal Chemistry, 2021, 211, 113005.	5.5	8
106	Cross-validation study between the HRRT and the PET component of the SIGNA PET/MRI system with focus on neuroimaging. EJNMMI Physics, 2021, 8, 20.	2.7	8
107	Dopaminergic Positron Emission Tomography Imaging in the Alpha‣ynuclein Preformed Fibril Model Reveals Similarities to Early Parkinson's Disease. Movement Disorders, 2022, 37, 1739-1748.	3.9	8
108	Cutting-Edge Brain Imaging with Positron Emission Tomography. Neuroimaging Clinics of North America, 2007, 17, 427-440.	1.0	7

#	Article	IF	CITATIONS
109	Impact of Contamination from Scattered Photons in Singles-Mode Transmission Data on Quantitative Small-Animal PET Imaging. Journal of Nuclear Medicine, 2008, 49, 1852-1861.	5.0	7
110	Functional neuroimaging in Parkinson's disease. Expert Opinion on Medical Diagnostics, 2011, 5, 109-120.	1.6	7
111	Simulation guided optimization of Dual Layer Offset detector design for use in small animal PET. , 2011, , ,		7
112	Evaluation of very highly pixellated crystal blocks with SiPM readout as candidates for PET/MR detectors in a small animal PET insert. , 2012, , .		7
113	Advances in PET Methodology. International Review of Neurobiology, 2018, 141, 3-30.	2.0	7
114	PBB3 binding in a patient with corticobasal syndrome. Movement Disorders, 2018, 33, 1359-1360.	3.9	7
115	A PET detector interface board and slow control system based on the Raspberry Pi <sup>®</sup> . , 2013, , .		6
116	A familial form of parkinsonism, dementia, and motor neuron disease: A longitudinal study. Parkinsonism and Related Disorders, 2014, 20, 1129-1134.	2.2	6
117	Texture and shape analysis on high and low spatial resolution emission images. , 2014, , .		6
118	Interpreting <scp>DTBZ</scp> binding data in rodent: Inherent variability and compensation. Synapse, 2016, 70, 147-152.	1.2	6
119	Associations between cerebral amyloid and changes in cognitive function and falls risk in subcortical ischemic vascular cognitive impairment. BMC Geriatrics, 2017, 17, 133.	2.7	6
120	Measurement of energy and timing resolution of very highly pixellated LYSO crystal blocks with multiplexed SiPM readout for use in a small animal PET/MR insert. , 2013, , .		5
121	Manganese concentration mapping in the rat brain with MRI, PET, and autoradiography. Medical Physics, 2017, 44, 4056-4067.	3.0	5
122	Basal Ganglia Studies with 3D Acquisition and 2D Reconstruction on a Retractable Septa PET Scanner. Journal of Computer Assisted Tomography, 1994, 18, 1004-1009.	0.9	4
123	Pixelated Geiger-Mode Avalanche Photo-Diode Characterization Through Dark Current Measurement. IEEE Transactions on Nuclear Science, 2014, 61, 1369-1375.	2.0	4
124	Characterization of a Small Animal PET Detector Block Incorporating a Digital Photon Counter Array. IEEE Transactions on Nuclear Science, 2015, 62, 732-739.	2.0	4
125	Imaging in Neurodegeneration: Movement Disorders. IEEE Transactions on Radiation and Plasma Medical Sciences, 2019, 3, 262-274.	3.7	4
126	Novel data-driven, equation-free method captures spatio-temporal patterns of neurodegeneration in Parkinson's disease: Application of dynamic mode decomposition to PET. NeuroImage: Clinical, 2020, 25, 102150.	2.7	4

#	Article	IF	CITATIONS
127	Detection of transient neurotransmitter response using personalized neural networks. Physics in Medicine and Biology, 2020, 65, 235004.	3.0	4
128	Cutting-Edge Brain Imaging withÂPositron Emission Tomography. PET Clinics, 2007, 2, 91-104.	3.0	3
129	Data Acquisition for a Preclinical MR Compatible PET Insert Using the OpenPET Platform. IEEE Transactions on Radiation and Plasma Medical Sciences, 2017, 1, 495-504.	3.7	3
130	Effect of Dopamine D <sub>2</sub> Receptor Antagonists on [ <sup>18</sup> F]-FEOBV Binding. Molecular Pharmaceutics, 2020, 17, 865-872.	4.6	3
131	A Clobal and a segmented plane scatter calibration: improving the quantitative accuracy of frames with high random fraction and/or low number of counts in dynamic high resolution PET brain imaging. , 2007, , .		2
132	Analytical modeling and implementation of detector response for fully 3D computer simulation and image reconstruction of an MRI compatible PET insert with a dual-layer offset crystal design. , 2012, , .		2
133	A simple route to [11C]N-Me labeling of aminosuberic acid for proof of feasibility imaging of the xCâ^' transporter. Bioorganic and Medicinal Chemistry Letters, 2014, 24, 5512-5515.	2.2	2
134	Evaluation of performance and stability of an MR compatible PET detector. , 2014, , .		2
135	Development of a digital unrestrained mouse phantom with non-periodic deformable motion. , 2015, , .		2
136	Denoising and DA release: effect of denoising on the ability to identify voxel-level neurophysiological response. , 2018, , .		2
137	Modeling of [18F]FEOBV Pharmacokinetics in Rat Brain. Molecular Imaging and Biology, 2020, 22, 931-939.	2.6	2
138	Electron microscopy of antibody-conjugated, lutetium-177 lanthanide gold-coated nanoparticles: Proof of concept of targeted loci—A potential theranostic agent. AIP Advances, 2021, 11, 045035.	1.3	2
139	A 4-D Iterative HYPR Denoising Operator Improves PET Image Quality. IEEE Transactions on Radiation and Plasma Medical Sciences, 2022, 6, 641-655.	3.7	2
140	Latest advance in the scatter calibration and combining the scatter calibration with a practical scatter and random approximation technique for dynamic brain imaging in high resolution PET. , 2008, , .		1
141	Quality control protocol for frame-to-frame PET motion correction. , 2009, , .		1
142	Scanning rodents on the High Resolution Research Tomograph (HRRT) with point spread function reconstruction: A feasibility study. , 2010, , .		1
143	PET image reconstruction and motion correction using direct backprojection on point grids and clouds. , 2011, , .		1
144	Fully-automated segmentation of the striatum in the PET/MR images using data fusion. , 2012, , .		1

#	Article	IF	CITATIONS
145	PET image reconstruction with correction for non-periodic deformable motion!. , 2014, , .		1
146	Overexpression of HER-2 in MDA-MB-435/LCC6 Tumours is Associated with Higher Metabolic Activity and Lower Energy Stress. Scientific Reports, 2016, 6, 18537.	3.3	1
147	Resolution modeling in PET imaging: Theory, practice, benefits, and pitfalls. , 2013, 40, 064301.		1
148	Amyloidâ€independent vascular contributions to cortical atrophy and cognition in a multiâ€eenter mixed cohort with low to severe small vessel disease. Alzheimer's and Dementia, 2021, 17, .	0.8	1
149	Estimation of NECR, scatter fraction, and sensitivity of a new MR compatible small animal PET insert based on Monte-Carlo simulations. , 2012, , .		0
150	Feasibility of using geometric descriptors of tracer distribution for disease assessment. , 2014, , .		0
151	Reply to letter to the editor: Is there anything more to learn from SWEDD?. Movement Disorders, 2016, 31, 1426-1428.	3.9	0
152	A Monte Carlo approach for boosting transient dopamine release detection sensitivity. , 2019, , .		0
153	Denoising and DA release: application of the 4D denoised reconstruction HYPR4D-K-OSEM. , 2019, , .		0
154	Dopamine release during psychological stress in euthymic bipolar I disorder: a Positron Emission Tomography study with [11C]raclopride. Journal of Affective Disorders, 2021, 295, 724-732.	4.1	0
155	Comparison of Invasive and Non-invasive Estimation of [11C]PBR28 Binding in Non-human Primates. Molecular Imaging and Biology, 2022, 24, 404-415.	2.6	0
156	Cortical morphology predicts placebo response in multiple sclerosis. Scientific Reports, 2022, 12, 732.	3.3	0